

# Experimental and Numerical Investigation on the Heat Treatment Effects of AA6063 Aluminum Alloy Tubes during Rotary Draw Bending

Hamid Reza Rezaei Ashtiani\*, Shahab Moghaddam

\* hr\_rezaei@arakut.ac.ir & hrr.Ashtiani@gmail.com

School of Mechanical Engineering, Arak University of Technology, Arak, Iran

Received: January 2021

Revised: August 2021

Accepted: September 2021

DOI: 10.22068/ijmse.2066

**Abstract:** In this study, the effects of heat treatment of aluminum alloy on the tube bending process were investigated in the rotary draw bending process. As two experimental and numerical simulation methods were used to determine the wall-thinning, ovality, and spring back for extruded, annealed, and aged AA6063 aluminum alloy tubes in different bending angles and bend radii. Numerical simulations were done by the finite element method with Abaqus software. The results indicated that in comparison with annealed and extruded parts, wall-thinning reduced whereas the amount of ovality and spring-back increased in the aged tubes. Also, in each case, the percentage of wall-thinning decreased with increasing bend radius, and the effect of bend radius was greater in the reduction of ovality from the bending angle. Investigations showed that the spring-back rate also decreased with an increasing bending angle.

**Keywords:** Rotary draw tube bending, AA6063, Heat treatment, Wall-thinning, Ovality, Spring-back.

## 1. INTRODUCTION

The 6000 series' Aluminum alloys are widely used in various industries due to their high strength to weight ratios and suitable corrosion resistance. They have been applied in various industries such as aerospace, automobile, etc. These alloys are also used as a proper material in architecture design, transportation equipment, bicycle body, and welded structures. Hence, the estimation of their mechanical properties is important to ensure security in various applications [1]. Aluminum alloys in the 6xxx series generally include magnesium and silicon approximately in the percentage required for the creation of magnesium silicide ( $Mg_2Si$ ), that making them heat-treatable. This series of Al alloys comprise the highest volume of Al extruded products. AA6063 is a precipitation-hardened aluminum alloy that has appropriate strength, weldability, formability, and corrosion resistance. AA6063 can be remained in the solution heat-treated and strengthened by precipitation heat treatment (T6 heat treatment) after the solution [1, 2].

The tube bending process is widely used in the production of parts in the aerospace, automotive, and oil gas industries. Tubes are used as a part of many different industries. The range extends from home to advanced special components. The bending angle and the shape of the particular section are desired when tubes are used. Among

the various bending methods of the tube, the rotary draw tube bending method has high efficiency, accuracy, and flexibility. The bendability of tubes depends on geometric factors such as tube diameter and thickness and bend radius. Several defects such as wrinkling, spring back, ovality, and wall thinning can occur in the bending process [3-7]. In this regard, Wang and Kao presented an energy-based method to minimize the bending radius, which does not give wrinkling in the bending process. This method is a function of tube geometry and instrumental properties of matter [3]. Yang et al. examined the effects of bend radii and tube wall-thickness on the cross-sectional deformation and tube wall-thickness variation. They concluded that in compression areas, wrinkles appear that can be eliminated by adding a wiper die. It was also found that the clearance between the tube and wiper-die was an important factor in the appearance of wrinkling, so that if this value is less than 0.6 mm, then wrinkling occurs. The cross-sectional deformation and the reduction of the thickness increase when the bending radius is smaller and their research results showed that the cross-sectional shape is closer to the circle and wall-thickness reduction increases using mandrel [4]. Li et al. investigated a numerical simulation on the deformation behavior of a thin-walled tube with a large diameter under the bending process in small radii [5]. Yang and Zhan also conducted a study on the role of friction in the bending

behavior of thin-walled tubes in the rotating draw tube bending process in the range of small bending radii. They found that the greater friction between the tube and the pressure die, the variation in wall thickness and the deformation of the cross-section were reduced and, given the little impact on the wrinkle, it is recommended that more friction be applied between the tube and the pressure die, of course not to the extent that it causes scratches on the tube [6].

In addition to these factors, other factors also affect the rotating draw bending conditions. In this regard, the effects of temperature, bending speed and initial grain size on the bendability of tubes of AM30 magnesium alloy have been investigated by Wu et al. [7]. They reported that the cross-section ovality and released spring back rate decreased with increasing temperature, while the maximum wall-thinning rate reached the minimum at the moderate temperature. With increasing bending velocity, the wall-thinning rate and ovality increased, while the change of spring back rate exhibited an opposite trend. Moreover, the wall-thinning rate, spring back rate, and ovality increased with the growth of the initial grain size. Heng et al. investigated the role of the mandrel in the precision bending of thin-walled tubes. Based on this analysis, a 3D elastic-plastic FEM model of the NC bending process was established using the dynamic explicit FEM code ABAQUS/Explicit. The wrinkling in the tube NC bending process was conditional on the biaxial compressive stress state; the smaller the difference between the biaxial stresses was, the more possibility of wrinkling occurred. The research results helped to understand the mandrel's role in the improvement of forming limits and forming quality from point of plastic forming mechanism [8]. The effects of heat treatment on the mechanical properties and bendability of 6063 aluminum cold drawn tubes have been investigated by Bourget et al., The effects of time, temperature, and furnace heating rate were studied by them to identify an optimized heat treatment for tubes with different cold work level [9]. Engel and Hassan examined the effect of material properties on the rotary draw tube bending process with materials consisting of steel alloy 1.0036 and stainless steel alloy 1.4301. In this research, the calculation of the neutral axis shifting, wall thickness distribution, and longitudinal strains were presented using the

experimental tests and the FE simulation, as results showed that the neutral axis of the tube moved more towards the inner tube in steel alloy than in stainless steel tubes. Furthermore, the material properties influenced wall thickness distribution [10]. Zhang et al. conducted a study on the bending behavior of thin-walled titanium tubes with a large diameter and concluded that wrinkling is the most important behavior of titanium tubes during bending and it with increasing differences between the maximum wall-thickness increases and the minimum wall-thickness decreases, the tendency to wrinkling increases. Also, the bendability of the thin-walled titanium is very sensitive to the process parameters, and the wrinkling is also significantly affected by the mandrel diameter, while the reduction in wall-thickness is extremely affected by the clearance between the wiper die and tube [11]. The effect of some RDB parameters such as the pressure of pressure die, the boosting velocity of pressure die, friction between the tube and pressure die, mandrel position, and the number of mandrel balls were studied on the fracture, wrinkling, and tube's ovality by Safdarian [12]. The effects of process conditions to spring back of rotary draw bending (RDB) of rectangular H96 tube and sectional deformation were studied and compared using the simulation and the sensitivity analysis mathematical model by Zhu et al. [13]. the spring back behaviors of 6063 aluminum bent profiles in the whole manufacturing process were investigated by using FE analysis combined with experimental validation. In this research, the formation mechanism and rule of spring back for the aluminum profile at different process stages were determined and the optimum process route for manufacturing the bent aluminum profiles was proposed [14]. The influence of natural aging before and after the forming operation on spring-back was experimentally studied using rotary draw bending of a typical Al-Mg-Si alloy tube as the case by Ma et al. [15]. Through this work, a fundamental understanding of the influence of pre/post-aging on spring-back was provided, and they reported that the spring back angle of the T4 tempered AA6060 tube was more than twice that achieved for the fully-annealed tube during bending.

In this study, rotary draw bending (RDB) tests were carried out using 6063 aluminum alloy tubes with different microstructures, bending angles,

and radii. For this, tubes with different microstructures have been prepared by extrusion; annealing, and aging heat treatment to elucidate the influence of these parameters on the bendability of these materials. The effects of bending parameters (bending angle and bending radius) and heat treatment of AA6063 (extruded AA6063, AA6063-O, and AA6063-T6) on the thickness reduction, ovality, and spring back are studied using experimental and simulation. For this purpose, experiments and simulations are performed by tube bender machine and Abaqus software, respectively.

## 2. EXPERIMENTAL PROCEDURE

During the bending process, the bending moment induces axial forces in the inner and outer layers. The inner and outer layers are subjected to compressive and tensile stresses, respectively. This results in the thinning of the tube wall at the outer section of the curve and the thickening of the tube wall at the inner section of the curve. The wall-thickness reduction rate or the thinning degree ( $I_t$ ) is reported as  $I_t = \frac{t_0 - t}{t_0} \times 100(\%)$ . Where  $t_0$  is the initial thickness of the tube and  $t$  is the final minimum wall thickness on the extrados of the bent tube which is shown in Fig. 1(a).

As stated above, there is reluctance in both parts (outer and inner layer of the tube) to move toward the centerline. The outer layers tend to move toward the neutral side to reduce the percentage of elongation. This undesirable deformation of the cross-section of the bent tubes is indicated by the cross-section ovality ( $I_d$ ) that the amount of ovality is reported  $I_d = \frac{D_{\max} - D_{\min}}{D} \times 100(\%)$ . Where  $D$  is the initial diameter of the tube before the bending process,  $D_{\max}$  is the maximum tube diameter after bending while  $D_{\min}$  is the minimum tube diameter after bending (see Fig. 1(a) for details).

After the bending process is complete and the bent tube is removed from the bend die, the spring-back is appeared due to the elastic nature of the tube material. This is called the elastic recovery or spring back of the tube. During the bending process, the internal stresses are increased in the tube and upon unloading these stresses do not disappear. After bending the outer layer of the curve is subjected to tensile residual stress and the interlayer of the bend is subjected to compressive residual. These tensile and

compressive residual stresses create a pure moment that causes spring back. The spring-back amount of the tube depends on the bending angle and radius, tube size and material, mandrel, and tools. In practice, the amount of spring-back is calculated as  $I_\theta = \frac{\theta_0 - \theta}{\theta_0} \times 100(\%)$ . Where  $\theta_0$  is the bending angle before unloading and  $\theta$  is the bending angle after unloading (as shown in Fig. 1(b)).

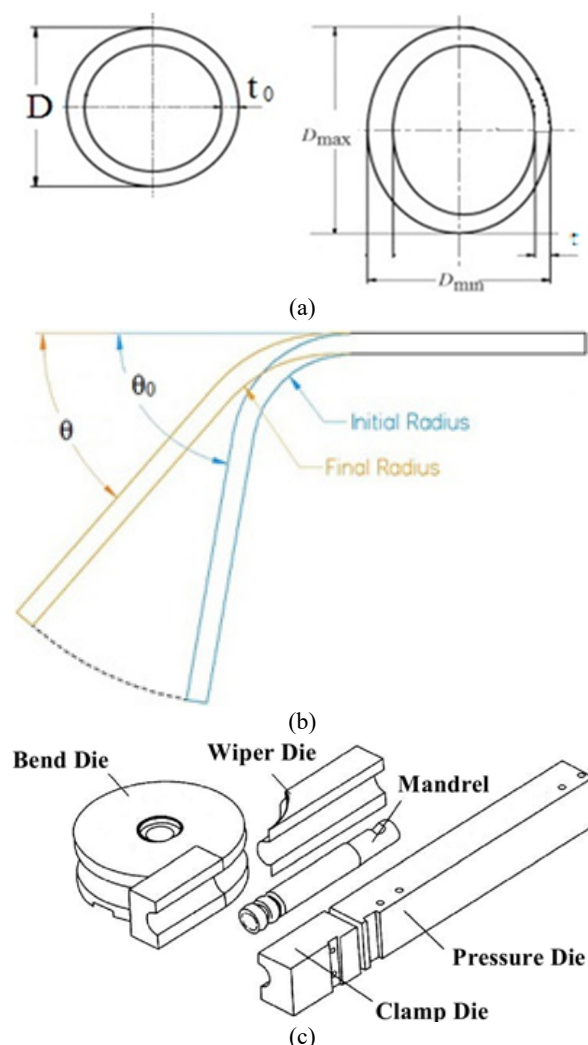


**Fig. 1.** Schematic of (a) wall-thinning and ovality, (b) spring-back, and (c) tooling setup for rotary draw tube bending.

As it is shown in Fig.1(c), the equipment of the rotary draw tube bending method includes bend, clamp, pressure, and wiper dies, and mandrel. In this method, the tube is firmly pressed into the bend die using the clamp die. The bend die rotates and pulls the tube in the desired bending degree and the bending radius. The pressure die prevents

the tube from rotating along with the bend die. The pressure die may be fixed or movable with the tube [16]. Mandrel prevents the wrinkling and collapse of the tube along with the wiper die.

AA6063 aluminum alloy was selected in this bending test since it offers a good combination of mechanical properties and weight. The chemical composition of this alloy is shown in Table 1. The geometric specifications of the tested tubes and also the bending radius and angles of the tests have been given in Table 2. In the bending process, the tube was clamped against the bend die to insert with the clamp die. The pressure die held the end of the tube against the wiper die as the bend die rotated and the tube was drawn forward. The bending tests were conducted at different bending radius and angles. The changes in wall thickness at tubes were measured along the axial direction by the ultrasonic thickness measurement device. Changes in the cross-section shape were evaluated by calculating the ovality, and the spring back rate was also measured after bending. The ovality and spring-back of the bent tubes were determined by using a digital caliper and goniometer, respectively. It is noted that the degree of reduction in thickness and ovality in each case is measured from the middle of the bend. All AA6063 tubes were extruded with homogenized ingots (AA6063-Ex) and to achieve different properties, as shown in Fig. 2, the tubes were subjected to different heat treatments of annealing (AA6063-O) and aging (AA6063-T6) after the extrusion process. Moreover, tensile test specimens were prepared according to the ASTM E08 standard to obtain the mechanical properties of all of the aluminum tubes and the true stress-strain curves of these samples consisting of AA6063-Ex, AA6063-O, and AA6063-T6 aluminum alloy have been given in Fig. 3.

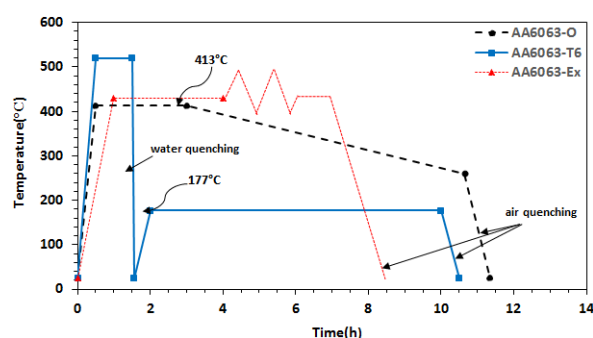


Fig. 2. Thermo-mechanical and heat treatment schematic used to prepare tube samples for the bending process.

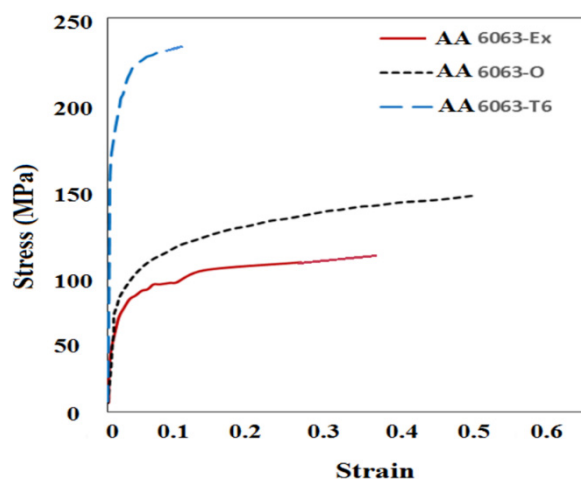


Fig. 3. Stress-strain curves of AA6063 with three different conditions.

### 3. FINITE ELEMENT MODELING

In this way, a 3-D elastic-plastic bending model has been constructed to simulate the rotary draw bending process for AA6063 aluminum alloy tubes using the commercial finite element (FE) software package, ABAQUS<sup>TM</sup> (Fig. 4), to predict the wall thickness distribution and reduction in wall-thickness, ovality and spring back.

Table 1. Chemical composition of AA6063 Aluminum alloy.

Element	Ti	Pb	Si	Fe	Cu	Mn	Mg	Cr	Zn	Al
Weight (%)	0.02	0.01	0.44	0.28	0.03	0.01	0.62	0.05	0.04	Bal

Table 2. Characteristics of the tube geometric and the bending process.

Parameter	Value
Tube Length	200 mm
Tube Diameter (OD)	20 mm
Tube Thickness	1 mm
Bending Radius(CLR)	32.5 mm, 40 mm, 55 mm
Bending Angle	45°, 90°, 135°

The FE models include the tube, tools, boundary constraints, and material properties. The tubes are assumed to be deformable solid and their elastic properties including Young's modulus, Poisson ratio, and density values were selected 65 GPa, 0.33, and 2700 kg/m<sup>3</sup>, respectively, and the ductile damage criteria are used as a ductile fracture model [17].

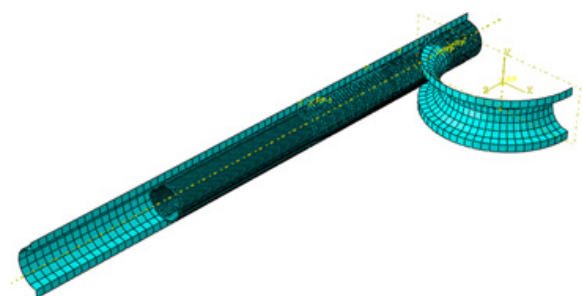


**Fig. 4.** 3D FE model for rotary draw bending process of AA6063 tubes.

The boundary constraints were determined following the real process of rotary draw bending. The bend, clamp, pressure, and wiper dies were constrained to rotate about the global y-axis simultaneously; the pressure die was constrained to translate only along the global z-axis; the wiper die was constrained along with all translation and rotation degrees of freedom. In the explicit simulation of the quasi-static bending process, the trapezoidal profile was used to define the smooth loading of all the dies to reduce inertial effects.

For the spring back simulation of the unloading process, proper constraints in no deformation zone were exerted to make sure that there was no rigid body rotation and translation. All simulations were performed with a fixed set of numerical parameters to investigate the effects of heat treatment of tubes on the bending behaviors and predict the wall-thickness, ovality, and spring back after unloading. Fig. 4 shows the toolset and initial tube before rotary draw bending. The tube mesh is C3D8R and the Coulomb friction criterion has been used for friction behavior and the type of contact on the surface to surface and also between the components. Friction coefficients between different surfaces are according to Table 3.

**Table 3.** Friction coefficients on various contact interfaces.

Surface	Friction coefficient
Tube Outside– Clamp Die	rough
Tube Outside– Bend Die	0.5
Tube Outside– Pressure Die	0.35
Tube Inside– Mandrel	0.1

#### 4. RESULTS AND DISCUSSION

The steps of the rotary draw bending process of aluminum alloy tubes using both experimental and simulation approaches have been shown in Figs. 5 (a) and (c), respectively.

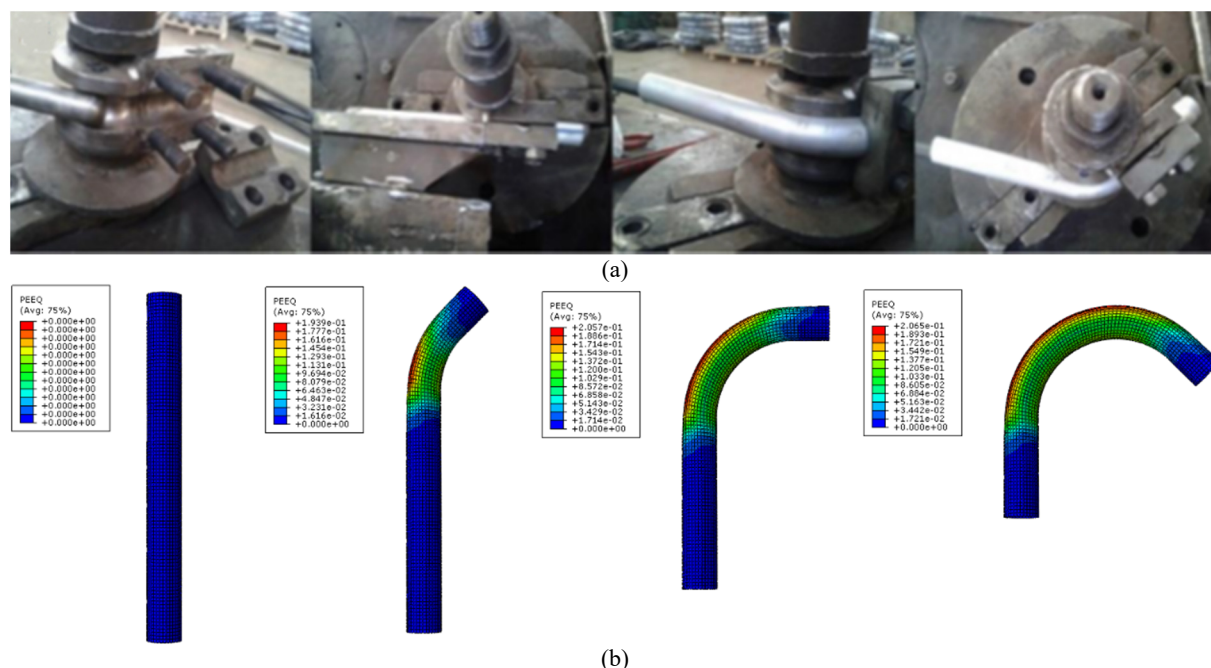


**Fig. 5.** Steps of the bending process of AA6063-O tubes in the (a) experimental and (b) simulation results.

The effects of bending parameters (bending angle and radius) and heat treatment of AA6063 (AA6063-Ex, AA6063-O, and AA6063-T6) on the thickness reduction, ovality, and spring back are studied using experiment and simulation approaches. The FE results are compared with the experimental ones to validate the FE simulation of RDB. The comparison of simulation and experimental results for the bent tube with a bending radius of 40 mm and a bending angle of  $135^\circ$  has been shown in Fig. 6.

The results show that the maximum mises stress is at the extrados of the bend. The comparison of the stress contours of AA6063-O tubes at the bending angle of  $135^\circ$  and for the different bending radius of 32.5, 40, and 55 mm have been shown in Figs.7 (a) to (c), respectively. As it is clear from these contours, the variation of the stresses along the cross-section from the intrados to the extrados of the bend. Besides, the stress at the crown location is not affected by the bend radius and equals the stress for a straight pipe. This behavior could be explained as when the bend is pressurized, the cross-section deforms into an oval shape with the major axis perpendicular to the plane of symmetry. The inner surface of the tube wall at the intrados and extrados will be subjected to compression bending stresses due to ovalization. However, the outer surface will be subjected to tensile stresses. The maximum value of stress is observed in the axial tensile stress brought by the internal

pressure could reduce the degree of compression at the intrados. The axial stresses at the intrados play a significant role in the initiation of wrinkling.

Fig. 8 shows the simulation stress contour of bent tubes with different materials in RDB tests at a bending radius of 55 mm and a bending angle of  $135^\circ$ . As this figure shows, the position of the region with high-stress values is changed by the RDB parameter variation. As it is clear, The AA6063-T6 tube withstands the most stress in a constant radius and bending angle, and then more stress is applied to the AA6063-O and AA6063-Ex tubes, sequentially. The reasons for this behavior are related to the microstructural and thus mechanical properties of tubes materials. The AA6063-T6 tube has more mechanical resistance against plastic deformation because of the high values of precipitations particles in its microstructures. The presence of this precipitation particle in the microstructure of AA6063-T6 aluminum alloys has been reported by other researchers [18] as the precipitations and secondary - phase particles of  $Mg_2Si$  were found in the microstructure of AA6063-T6 is more than of AA6063-O aluminum alloy. Therefore the results of the experimental and microstructural investigations show that the bendability of AA6063-Ex tubes is more than AA6063-O and AA6063-T6 tubes whereas AA6063-T6 tubes have the lowest bendability compared to other investigated aluminum alloy tubes.

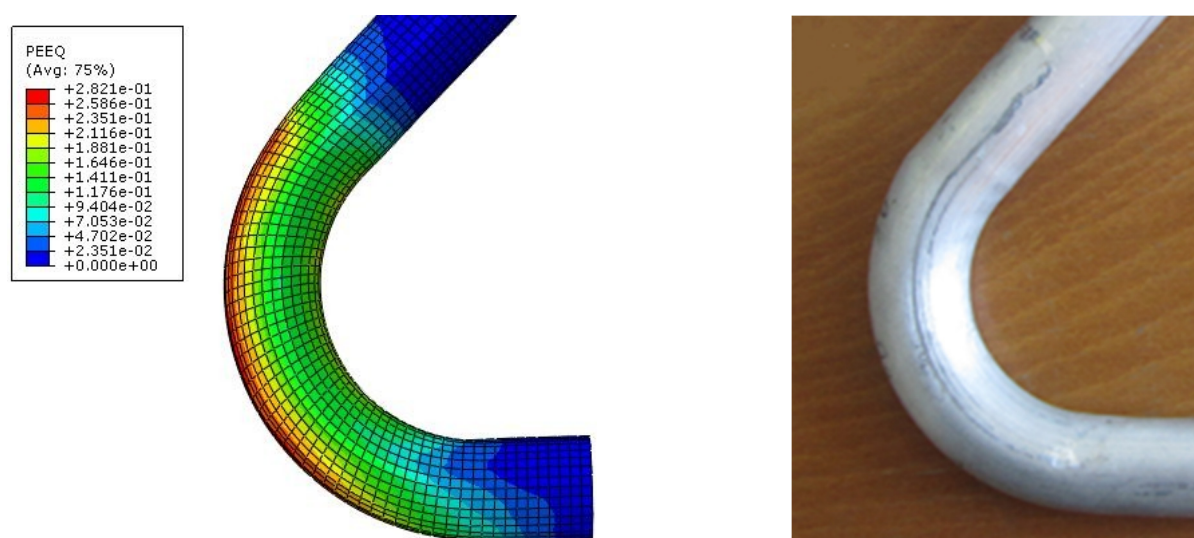


**Fig. 6.** Simulation and experimental bending results of AA6063-O tubes for a bending radius of 40 mm and a bending angle of  $135^\circ$ .

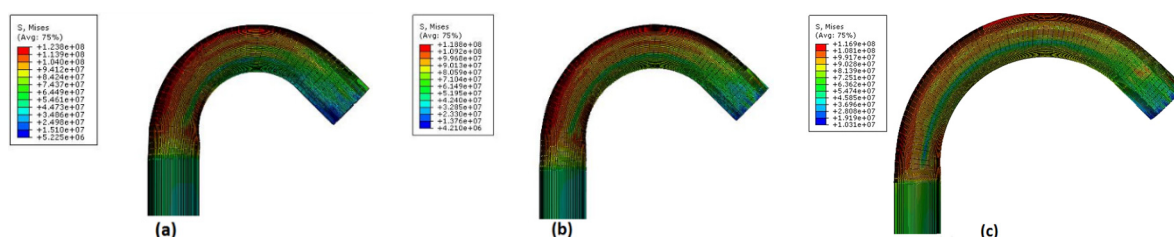


**Fig. 7.** A comparison of the von mises stresses contours of AA6063-O tubes materials at the bending angle of 135° and for the different bending radius of (a) 32.5, (b) 40, and (c) 55 mm.

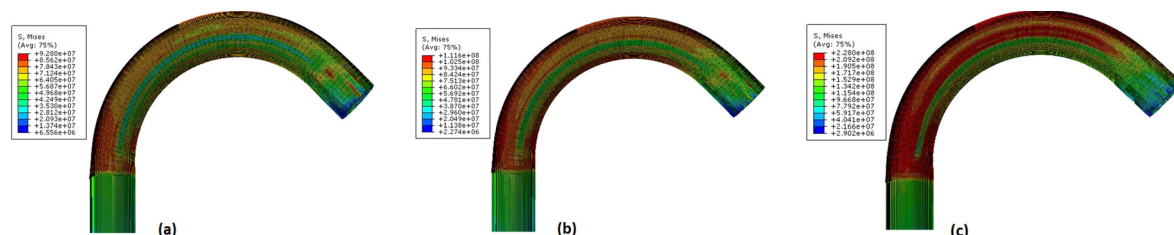


**Fig. 8.** Comparison of the von-mises stresses contour of different tubes of (a) AA6063-Ex, (b) AA6063-O, and (c) AA6063-T6 with a bending radius of 55 mm and a bending angle of 135°.

#### 4.1. Wall-thinning

As it is clear from Fig. 9, the wall-thinning of bent tube increases with increases in bending angle and decreases in bending radius.

As shown in Fig. 10, the aged tubes (AA6063-T6) were ruptured due to a decrease in the percentage of formability in comparison to other applied aluminum alloys tubes at the bending radii of 32.5 and 40 mm.

The results show that the wall thinning degree of the AA6063-T6 tube is the lowest value compared to other AA6063 alloys tubes with a bending radius of 55mm.

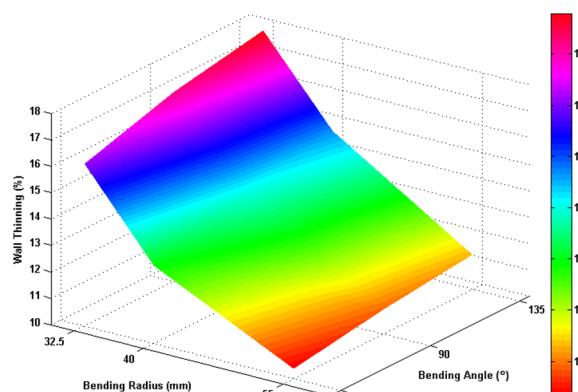


**Fig. 9.** Profile of wall thinning degrees of bent AA6063-Ex tube at different bending angles and radius using the FE simulation.

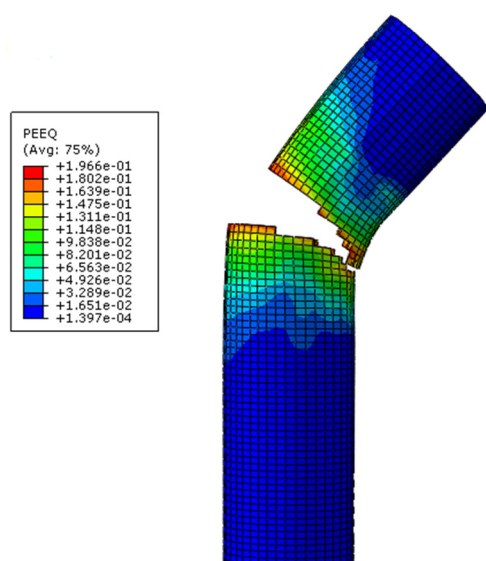


**Fig. 10.** Fractured AA 6063-T6 tube after (a) simulation and (b) experimental bending test at a bending radius of 32.5 mm.

Figs. 11(a) and (b) and 12 show the comparisons of FE simulation and experimental wall thinning degrees with the different applied heat treatment of AA6063 and bending angles at the different bending radius of 32.5, 40, and 55 mm, respectively. It is found that the wall thinning degree increases when the bending angle rises at different bending radius and microstructure of the AA6063 tube. Also, it is clear that the wall thinning degree of the AA6063-O tube is greater

than its AA6063-EX tube all over the stable bending process with a bending radius of 32.5 mm and 40 mm, whereas the AA6063-T6 tube was failed during rotary draw bending with these bending angles values.

Fig. 12 shows that the lowest value of the wall thinning degree belongs to the AA6063-T6 tube during rotary draw bending at all of the bending angle values and the bending radius of 55 mm.

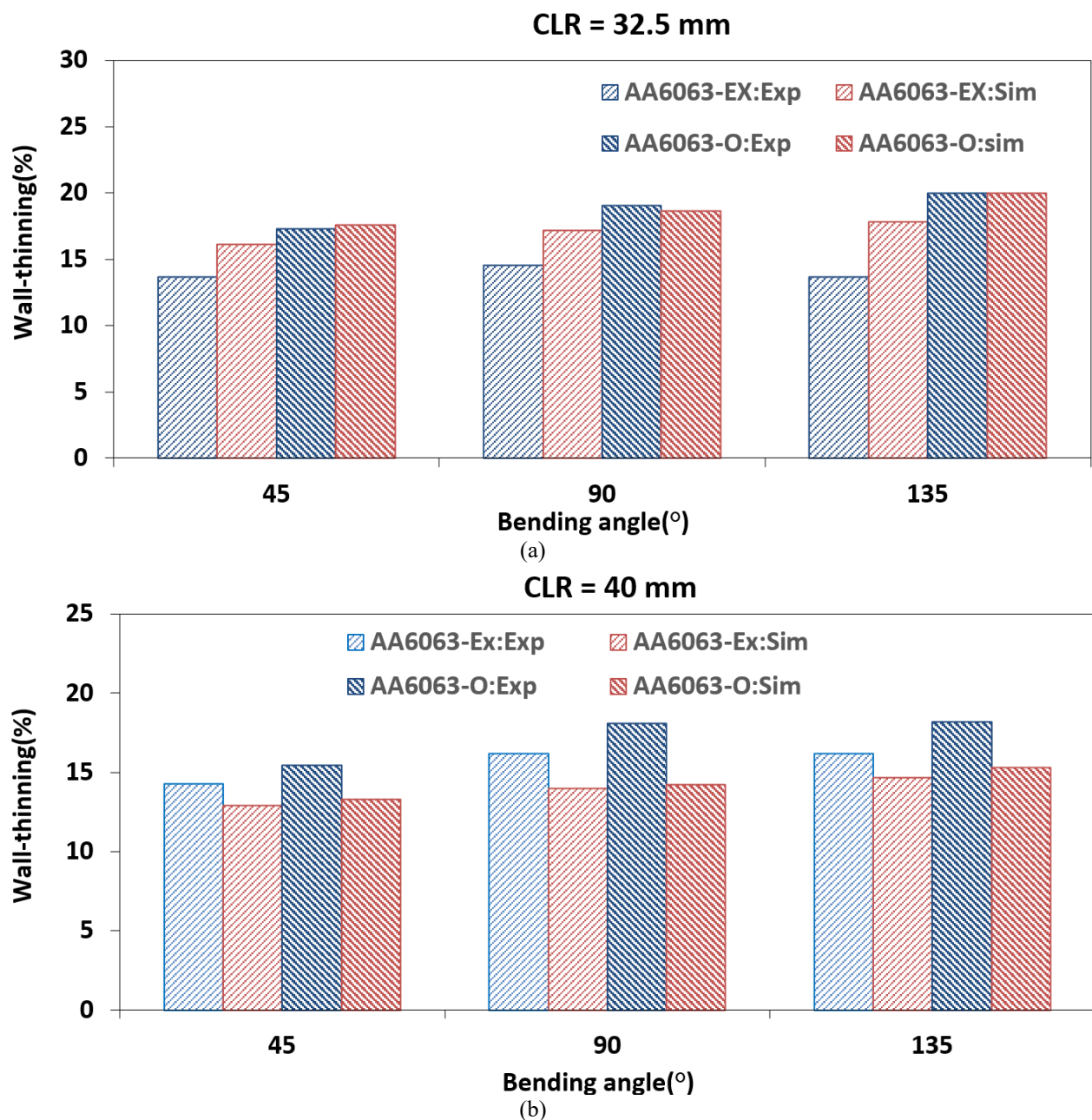
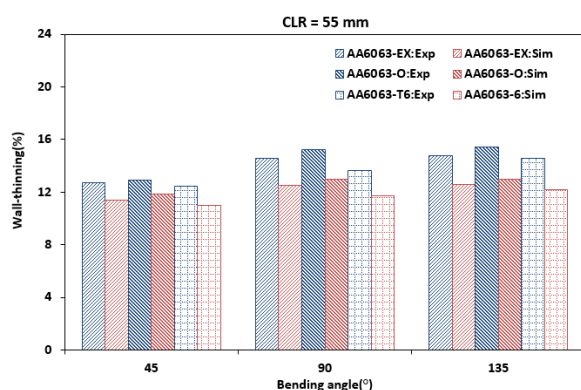


Fig. 11. Comparison of experimental and simulation results of wall thinning between AA6063-Ex and AA6063-O tubes at a bending radius of (a) 32.5 mm, and (b) 40 mm.

As it is clear from the experimental and simulation results, the FE simulation results still coincide with the experimental results for all of the aluminum alloy tubes and bending angle and radius. In terms of the wall thinning degree, it is found that the relative error between experimental and simulation results is less than 16% and the absolute error is about 3.6%; thus, the developed FE model is validated and can be used to further research the bending angle and radius in bending deformation of RDB. So the tube can be bent stably on the above conditions.



**Fig. 12.** Comparison of experimental and simulation results of wall thinning of AA6063-EX, AA6063-O, and AA6063-T6 tubes at a bending radius of 55 mm.

## 4.2. Ovality

It is experimentally found that the cross-section distortion degree of the mid-cross-section is almost maximum among the distortion degrees of tube cross-sections and ovality is one of the deformation phenomena of the bent tube. Fig. 13 shows the comparison of FE wall thinning and ovality with experimental ones in the middle part of the tube. It is found that the FE simulation model is properly validated by the experiment. The results show that the ovality of the bent tube decreases with increasing the bending radius at a constant bending angle (see Fig. 14). Therefore, the bending radius has a great influence on the ovality in the rotary draw tube bending process. As reported earlier, the aged alloy (AA6063-T6) tubes were ruptured due to reduced elongation and formability in the bending radius of 32.5 and 40 mm. Based on the present experimental and simulation results, it is concluded that the ovality increases with increasing bending angle in the bending radius of 32.5 mm (Fig. 15 (a)). Whereas the ovality values decrease with increasing

bending angles in the bending radius of 40 mm and 55 mm (Fig. 15 (b) and (c)). Fig. 15 (c) shows the comparisons of FE simulation ovality with experimental ones with different bending angles and the different heat treatment of AA6063 consisting of Extruded (AA6063-Ex), Annealed (AA6063-O), and Aged (AA6063-T6) tubes, respectively, at the bending radius of 55 mm.

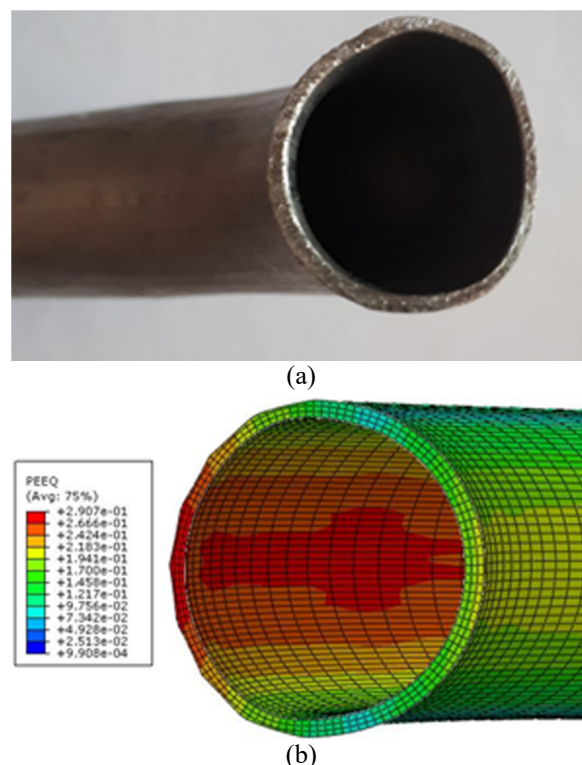


**Fig. 13.** Wall-thinning and ovality in the middle part of the tube in (a) experimental and (b) simulation results.

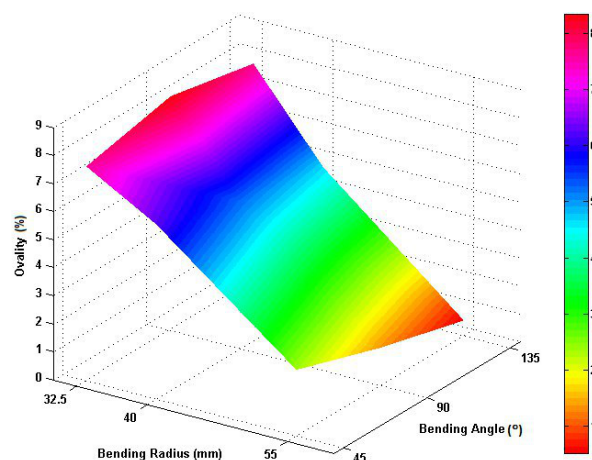


**Fig. 14.** Ovality changing of AA6063-Ex tubes for different values of the bending radius and angles in simulation tests.

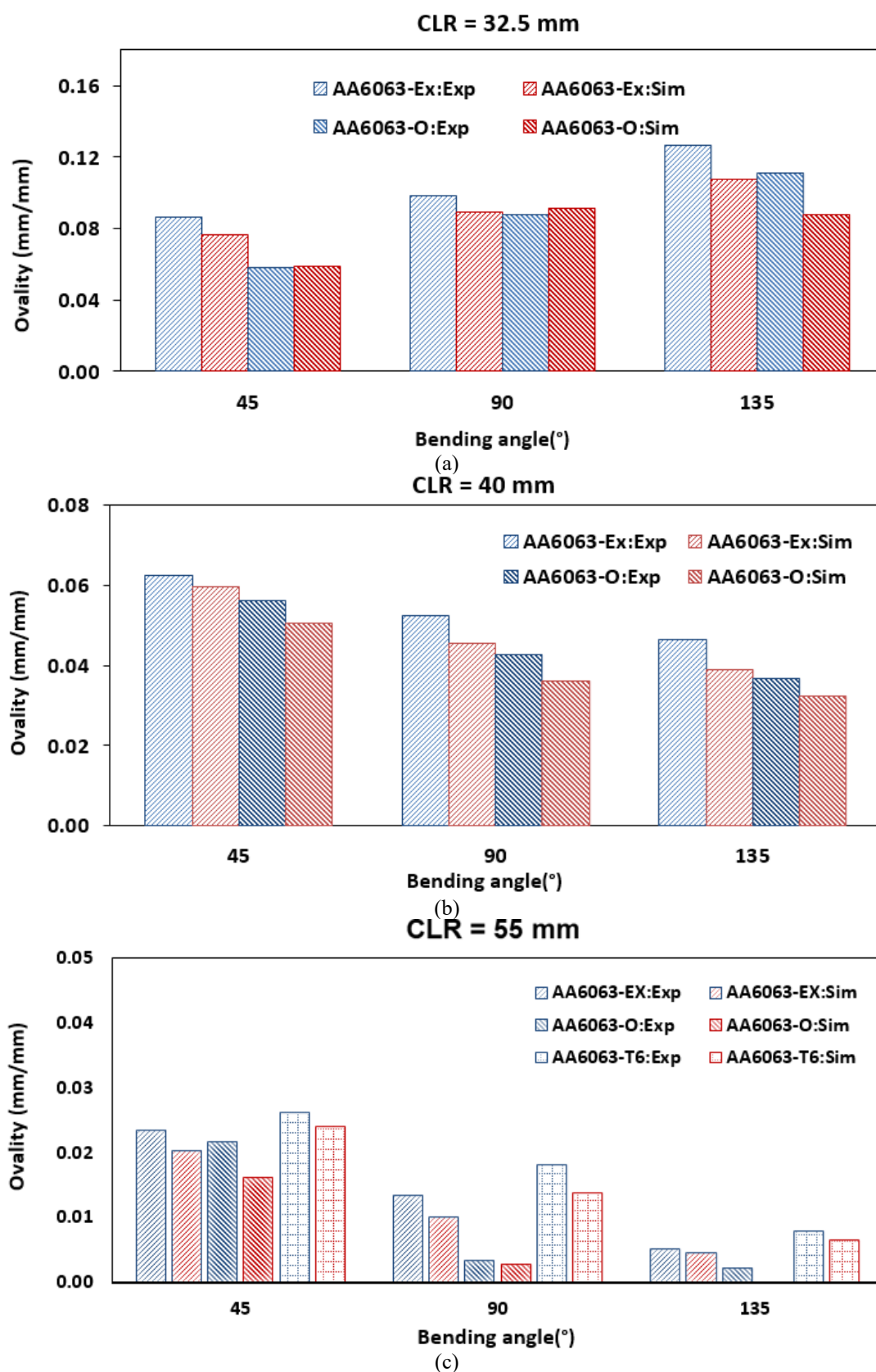


**Fig. 15.** Comparison of experimental and simulation ovality results of AA6063-Ex, AA6063-O, and AA6063-T6 tubes at a bending radius of (a) 32.5, (b) 40, and (c) 55 mm.

As it is clear in this figure, the ovality of the bent tube increases slightly with decreasing bending angle. Simulations and experimental results show that the heat treatment of AA6063 has a significant effect on the amount of ovality through-thickness of the bent tube.

It is found that the maximum ovality occurs for AA6063-T6, AA6063-Ex, and AA6063-O tubes, consecutively, in a specific bending angle and radius.

### 4.3. Spring-back

The spring back can be approximated from the sheet thickness, elasticity modulus, yield strength, and also bending process parameters such as the bend angle and radius. The effects of bending angle and radius on the experimental values of spring-back of bent AA6063-Ex tube have been shown in Fig. 16. It is obvious that the spring-back is affected by the conditions of tube bending deformation, as the spring-back decreases with increasing of the bending angle for any radius of the bend.

It can be seen from this figure that the spring-back decreases with increasing the bending angle in all radii.

It is also observed that in a constant bending angle, the spring-back increase with increasing the bending radius, this is due to the fact that with increasing bending radius, the plastic deformation region decreases relative to the elastic region, thus, the increase in the elastic region increases the spring-back. So, spring back decreases with decreasing the relative bending radius.

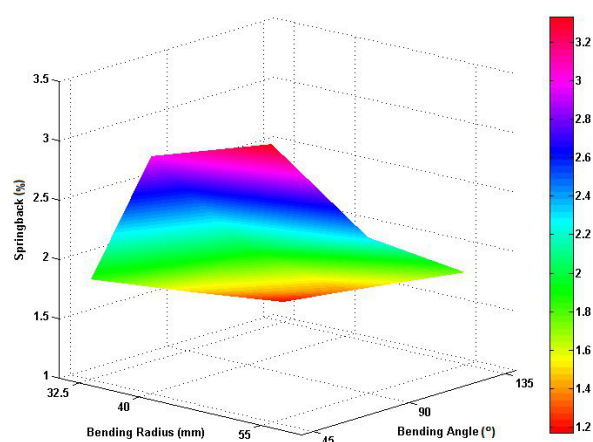


**Fig. 16.** Effects of bending radius and bending angle on the spring-back of AA 6063-Ex bent tubes.

The FE simulations and experimental results of the spring-back of bent tubes have been shown at different bending angles in Figs. 17 (a) to (c) with the bending radius of 32.5, 40, and 55 mm, respectively. The figures show good agreement in experimental and simulation results of spring-back of bent tubes.

The spring-back of the bent tube decreases with increasing the bending angle at different bending radius and heat treatment conditions of the AA6063 tubes and also it decreases with decreasing the bending radius. The results show that spring back is related to plastic deformation of the material, as spring-back decreases with increasing plastic deformation. It is clear from stress-strain curves of AA6063 alloys with different heat treatments in Fig. 3 that AA6063-T6, AA6063-O, and AA6063-Ex tubes have the maximum values of the resilient modulus, sequentially, therefore as it is obvious in Fig. 17 (c), the maximum spring-back value of tubes is owned by the AA6063-T6 tube and the spring-back value of the AA6063-O tube is greater than AA6063-Ex tube.

As it is clear in these results shown in Figs. 17 (a) and (b) that the spring-back have specified values all over the stable bending process with the bending radius of 32.5 mm and 40 mm, respectively, whereas the AA6063-T6 tube was failed during rotary draw bending with these bending radius values.

As shown in Fig. 17 (c), the extruded tubes have the lowest spring-back. Note that the aged tubes were ruptured due to reduced elongation and formability, due to bending radii of 32.5 mm and 40 mm.

The results show that the spring-back of the bent tube is significantly affected by the mechanical properties of the tubes materials and it decreases with increasing the bending angle values and decreasing the bend radius. In terms of the spring back rate, it is found that the relative error between experimental and simulation results is less than 14%, the developed FE model can be used to further research the bending angle and radius in bending deformation of RDB.

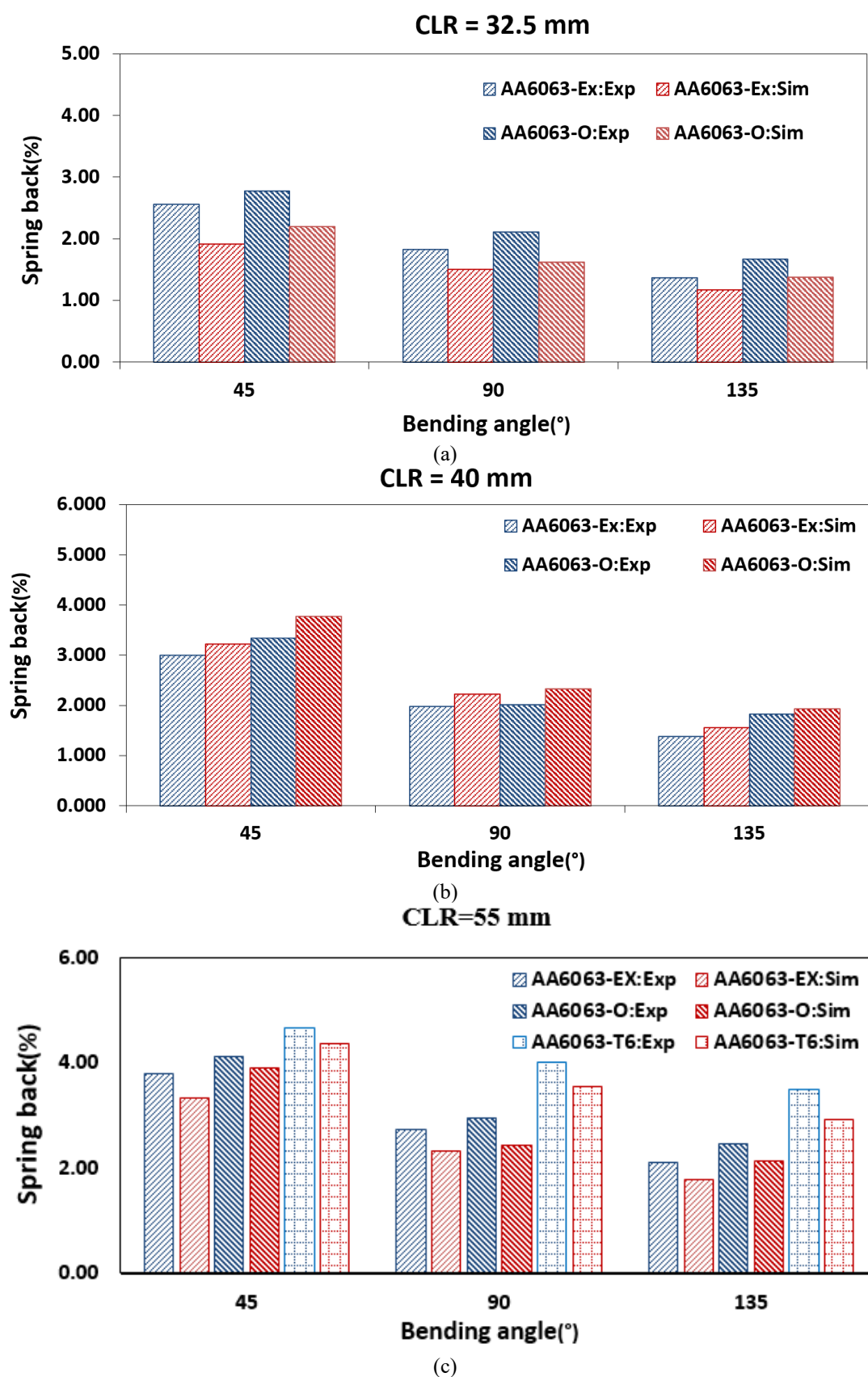


**Fig. 17.** Comparison of experimental and simulation results of spring-back for A6063-Ex, AA6063-O, and AA6063-T6 tubes at the bending radius of (a) 32, (b) 40, and (c) 55 mm.

## 5. CONCLUSION

In this work, the experimental and numerical study was done on the rotary draw bending of AA6063 aluminum alloy tubes consisting of three conditions: extruded, annealed, and aged AA6063 alloy tubes. The FEM was used to predict some of the defects such as fracture, wall thinning, ovality, and spring-back of tubes in the RDB process by using Abaqus/Explicit combined with experimental validation. It was found that:

- The heat treatment of the AA6063 aluminum alloy tube has a significant effect on the defects such as wall thinning, ovality, and spring-back of tubes in the RDB process, as the AA6063-T6 tube has the highest amount of ovality and spring-back.
- The wall thinning increases with increasing bending radius and decreasing bending angle. Therefore, the radius of the bend must be larger and the bending angle is considered smaller to minimize wall thinning degree. Also, the AA6063-T6 tube has the lowest wall thinning degree values in comparison to other AA6063 alloys tubes with a suitably selected bending radius.
- The ovality decreases with increasing bending angle slowly and increasing the bending radius faster. The effects of the bending radius are greater in reducing the ovality from the bending angle. Therefore, the bending radius should be increased as much as possible to reduce ovality. Also, the heat treatment of AA6063 has a significant effect on the amount of ovality through-thickness of the bent tube, as in a specific bending angle and radius, the maximum ovality occurs for AA6063-T6, AA6063-Ex, and AA6063-O tube, sequentially.
- The spring-back decreases with increasing the bending angle at a constant bending radius and with a decreasing bending radius. Therefore, to minimize the spring-back, the bending angle must be larger and the bending radius must be smaller. The maximum amount of spring-back is owned by the AA6063-T6 tube and the spring-back of the AA6063-O tube is greater than the AA6063-Ex tube.

## REFERENCES

- [1] G. Das, M. Das, S. Ghosh, P. Dubey, A.K. Ray, Effect of aging on mechanical

properties of 6063 Al-alloy using instrumented ball indentation technique, *Mater. Sci. Eng. A.*, 527, 2010, 1590–1594. <https://doi.org/10.1016/j.msea.2009.10.037>.

- [2] Khadyko, M., O. R. Myhr, and O. S. Hopperstad. "Work hardening and plastic anisotropy of naturally and artificially aged aluminium alloy AA6063.", *Mechanics of Materials* 136, 2019: 103069. <https://doi.org/10.1016/j.mechmat.2019.103069>.
- [3] X. Wang, Wrinkling Limit in Tube Bending, *J. Eng. Mater. Technol.*, 123, 2013. <https://doi.org/10.1115/1.1395018>.
- [4] J. Yang, B. Jeon, S. Oh, The tube bending technology of a hydroforming process for an automotive part, *J. Mater. Process. Technol.*, 111, 2001, 175–181.
- [5] H. Li, H. Yang, J. Yan, M. Zhan, Numerical study on deformation behaviors of thin-walled tube NC bending with large diameter and small bending radius, *Comput. Mater. Sci.*, 45, 2009, 921–934. <https://doi.org/10.1016/j.commatsci.2008.12.018>.
- [6] H. Yang, H. Li, M. Zhan, Journal of Materials Processing Technology Friction role in bending behaviors of thin-walled tube in rotary-draw-bending under small bending radii, *J. Mater. Process. Technol.*, 210, 2010, 2273–2284. <https://doi.org/10.1016/j.jmatprotec.2010.08.021>.
- [7] W. Wu, P. Zhang, X. Zeng, L. Jin, S. Yao, A.A. Luo, Bendability of the wrought magnesium alloy AM30 tubes using a rotary draw bender, *Mater. Sci. Eng. A.*, 486, 2008, 596–601. <https://doi.org/10.1016/j.msea.2007.09.033>.
- [8] L. Heng, Y.H. Å, Z. Mei, S. Zhichao, G. Ruijie, Role of mandrel in NC precision bending process of thin-walled tube, *Int. J. Mach. Tools Manuf.*, 47, 2007, 1164–1175. <https://doi.org/10.1016/j.ijmachtools.2006.09.001>.
- [9] J. Bourget, M. Fafard, H.R. Shakeri, T. Côté, Journal of Materials Processing Technology Optimization of heat treatment in cold-drawn 6063 aluminium tubes, *J. Mater. Process. Technol. J.*, 209, 2009, 5035–5041. <https://doi.org/10.1016/j.jmatprotec.2009.01.027>.

- [10] I.S. Colloquium, The influence of material properties on rotary draw bending, in: 58th ILMENAU Sci. Colloq. Tech. Univ. Ilmenau, 08 – 12 Sept. 2014 URN Urnbndegbvilm1-2014iwb3, 2014: 8–12.
- [11] Z. Zhang, H. Yang, H. Li, N. Ren, Y. Tian, Bending behaviors of large diameter thin-walled CP-Ti tube in rotary draw bending, *Prog. Nat. Sci. Mater. Int.*, 21, 2011, 401–412. [https://doi.org/10.1016/S1002-0071\(12\)60076-8](https://doi.org/10.1016/S1002-0071(12)60076-8).
- [12] Safdarian, R. Investigation of tube fracture in the rotary draw bending process using experimental and numerical methods. *Int J Mater Form*, 13, 493–516, 2020. <https://doi.org/10.1007/s12289-019-01484-5>
- [13] Zhu, Y. X., Chen, W., Li, H. P., Liu, Y. L., & Chen, L. 2018, Springback study of RDB of rectangular H96 tube. *International Journal of Mechanical Sciences*, 138–139, 282–294. <https://doi.org/10.1016/j.ijmecsci.2018.02.022>.
- [14] Liu, Z., Li, L., Wang, G., Chen, J., & Yi, J. Springback behaviors of extruded 6063 aluminum profile in subsequent multi-stage manufacturing processes. *The International Journal of Advanced Manufacturing Technology*, 109(1), 2020, 1-13. <https://doi.org/10.1007/s00170-020-05551-z>.
- [15] Ma, J., Ha, T., Blindheim, J., Welo, T., Ringen, G. and Li, H., Exploring the Influence of Pre/Post-Aging on Springback in Al-Mg-Si Alloy Tube Bending. *Procedia Manufacturing*, 47, 2020, 774-780. <https://doi.org/10.1016/j.promfg.2020.04.239>.
- [16] Agarwal, R., Tube bending with axial pull and internal pressure, Master Thesis, Texas A&M University, Texas, 2004.
- [17] Jafarlou, D.M., Zalnezhad, E., Hamouda, A.S. et al. Evaluation of the Mechanical Properties of AA 6063 Processed by Severe Plastic Deformation. *Metall Mater Trans A*, 46, 2015 2172–2184. <https://doi.org/10.1007/s11661-015-2806-7>.
- [18] Mohammadi M, Rezaei Ashtiani H., Influence of Heat Treatment on the AA6061 and AA6063 Aluminum Alloys Behavior at Elevated Deformation Temperature. *Iranian Journal of Materials Science and Engineering*. 18(2), 2021. <https://doi.org/10.22068/ijmse.1890>.